Dynamic Analysis and Design of the SIRTF Primary Mirror Mount

Ralph M. Richard, Principal Investigator

Daniel Vukobratovich, Co-principal Investigator

and

L. Wayne Pollard

Optical Sciences Center

University of Arizona

Tucson, Arizona 85721

Prepared for

NASA Ames Research Center

Space Technology Branch 244-7

Moffett Field, California 94035

June 1985 - Sept. 1986

NASA Grant No. 2-220

FINAL REPORT

TABLE OF CONTENTS

Introduction 1

Flexure Design Criteria 2

Mount Design Considerations 3

Description of Mount Design 7

Structure Modeling for Dynamic Analysis 9

Summary 48

Appendix 49

References 53

INTRODUCTION

Under a prior grant from the NASA Ames Research Center, the University of Arizona Optical Sciences Center (OSC) developed a 0.5-m fused-silica lightweight double-arch mirror-and-flexure mount as a candidate technology for the Space Infrared Telescope Facility (SIRTF) primary mirror (1). Three developmental efforts were made: 1) the design of a lightweight double-arch fused-silica mirror, 2) a glass-to-metal transition device (in this case a socket and T-clamp), and 3) a flexure mount with radial compliance to accommodate the effects of cryogenic contraction of the baseplate and fabrication tolerances on the optical figure of the mirror. These developmental activities used finite-element modeling to guide the actual design. Following the analytical effort, a test 0.5-m fused-silica mirror and mount were fabricated at the OSC.

This 0.5-m test mirror and mount have now been evaluated at the NASA-Ames cryogenic test facility. A cryogenic distortion of 0.1 waves rms at 633 nm at a test temperature of 7.9 K resulted. This is a very promising result for demonstrating the feasibility of a glass primary mirror for SIRTF.

The existing 0.5-m mirror and mount were not analyzed or designed for the loads induced during shuttle launch because of the absence of information on these dynamic loads as well as lack of resources at the OSC with given budget and time constraints.

Using shuttle launch loadings provided by the NASA Ames SIRTF Technology Staff, a new flexure-gimbel mount and mirror socket for the 0.5-m test mirror was designed to survive the shuttle launch load environment in addition to meeting both cryogenic and fabrication constraints on the optical quality of the mirror.

A candidate baseplate, flexure, gimbal and socket design was also studied for the full scale test mirror.

FLEXURE DESIGN CRITERIA

The baseline SIRTF telescope design is a 0.85 m diameter, f/2.4 Ritchey-Chretien. The primary mirror mount for the telescope must meet the following criteria:

1. The mirror must be held within the alignment tolerances of the telescope following insertion into orbit. The mount must allow alignment on the ground with the exception of correcting the spacing between primary and secondary mirrors; in orbit alignment was not considered.

The tolerance for system decenter (from ref. 1) is 0.023 waves (one wave = 633 nm), for despace 0.036 waves, and for tilt 0.39 waves. These tolerances can be translated into physical displacements of the primary mirror using equations developed by Wetherel (Ref. 2). Allocating half of these tolerances to the primary, the despace permitted is 135 μm, the allowable decenter is 30 μm, and maximum tilt is 167 μrad.

Three alignment cases are considered: the static "1 g" on the ground test, alignment following cooldown, and alignment following orbital insertion. Alignment error due to gravity when the system is in its test position must be less than the above tolerances. The cooldown case is one of dealing with a mismatch in thermal coefficients of expansion between the mirror and its mount. Misalignment due to acceleration and vibration loads during launch can exceed the tolerances, providing that the mirror returns to the correct position following orbital insertion.

2. The mirror optical surface must not be distorted by the mount during cooldown by more than the figure error tolerance. Until recently the mount induced figure error was budgeted at 0.077 waves; recently this tolerance has been relaxed to 0.146 waves.

3. The mount must safely retain the mirror during an emergency landing of the shuttle. Anticipated loads in this case are 4.5 g in all axes. Misalignment following an emergency landing is permissible.

4. The mount must use as little space and weight as possible. It must be very reliable and testable with confidence on the ground.

MOUNT DESIGN CONSIDERATIONS

The mirror mount selected for the SIRTF is dependent on the type of mirror and structure selected. In this study, a lightweight glass primary mirror was mounted in an aluminum telescope structure. The mount design maintains alignment of the mirror, and insures that contraction of the structure relative to the glass does not distort the mirror.

If despace is ignored and isothermal conditions exist, then the mount must deal with a radial contraction of the baseplate relative to the mirror when the system is cooled from room temperature to 10 K. A mount that permits contraction of the baseplate relative to the mirror, and that is stiff in all other directions is required.

The ideal thermal mount would have three rigid pegs attached to the mirror that slide freely in the radial direction, but constrain the mirror in all other directions. Relative motion between two components introduces friction by either sliding or rolling components.

For small angular rotation, on the order of 0.1 rad, ball bearings behave as lossy or nonlinear springs (Ref. 3). Friction varies from bearing to bearing as well as changes in position. This causes decenter and uneven radial forces on the mirror. Vibration and acceleration during launch could damage the bearings. It is also difficult to find lubricants and bearings qualified for reliable long life operation at 10 K in vacuum (Ref. 4).

Zero backlash and absence of friction make flextures ideal for the linear motion requirements of the mirror mount. Flexures eliminate the problems of wear and lubrication associated with conventional bearings and can be designed to operate in vacuum and at cryogenic temperatures.

Flexures have been used in the past to mount primary mirrors for space telescopes. Appendix I reviews this prior art. What is new is the extension of this technique to cryogenic temperatures and the type of flexure configuration.

In the past, mounts with the long axis of the flexures tangential to the mirror edge have been used in space telescopes. This configuration requires additional space in the telescope structure around the edge of the mirror. For a cylindrical tube telescope structure, the additional space requirement increases tube weight as the square of the mount diameter. When flexures are attached to the edge of the mirror, mount print through at the mirror edge significantly reduces the optical performance of the mirror. Since edge mounting requires additional mass at the mirror edge, the extra mass at the mirror edge has an unfavorable effect on the self-weight deflection of the mirror and increases the moment of inertia of the mirror.

Flexures mounted in sockets in the back of the mirror, with the long axis of the flexure parallel to the optical axis, avoid the problems of edge flexures whereas back mounted flexures increase the telescope structure length. Since structural weight increases linearly with length, this is less serious than that of edge mounted flexures. Back mounted flexures which can be located at the optimum support points form minimum self-weight induced deflection of the mirror. This allows the mirror to be tested in its fabricated support. Mount print through at these location is less serious.

Two requirements are important in the design of the mount flexures: the flexures must be stiff in all but the radial direction, where high compliance is desired, and it must be possible to fabricate the flexures. The stiffness requirement comes from the random vibration that the mirror and mount experience during launch. This requirement can be relaxed if a caging mechanism is used to lock up mirror and mount during launch. A caging mechanism is considered undesirable for this application since it is an additional, active mechanism that could fail, compromising the optical performance of the system. The fabrication requirement is driven by experience. This requirement sets limits on the physical dimensions of the flexures as well as the precision of fabrication.

To survive launch, the flexure and mount system should have fundamental frequencies high enough to be on the low portion of the random vibration curve.

Keeping the fundamental frequencies high means keeping the flexures stiff. Each of the mount flexures can be either a single blade (used on IRAS) or a double bladed parallel spring guide (developed in prior work on this contract).

Consider first a parallel spring guide. In the absence of an axial force on the flexures (the in orbit case), the radial compliance is given by:

$$\frac{\delta}{F} = \frac{L^3}{2Ebt^3} \tag{1}$$

where:

δ is the radial deflection
F is the radial force applied to the flexure
L is the flexure length
E is the flexure material elastic modulus
b is the flexure width in the tangential direction
t is the flexure thickness in the radial direction

The maximum stress in the flexure is given by:

$$\sigma = \frac{3FL}{2bt^2} \tag{2}$$

where:

σ is the maximum stress

Combining Eqs. 1 and 2, the expression for the compliance becomes:

$$\frac{\delta}{F} = \left[\frac{\sigma}{E}\right]\left[\frac{t}{3F}\right]\left[\frac{L}{t}\right]^2 \tag{3}$$

The ratio of the allowable stress to the elastic modulus is known as the reduced tensile modulus. For maximum radial compliance at a given flexure length, this ratio should be as high as possible so that the best flexure material has the highest reduced tensile modulus. A high allowable stress and a low elastic modulus are desirable. Alternately, combining Eqs. 1 and 2 and solving for the length L:

$$L = \sqrt{3\delta t\left[\frac{E}{\sigma}\right]} \tag{4}$$

Since the deflection is set by the contraction of the baseplate during cooldown, the thickness of the flexure must be small for minimum flexure length which is set by fabrication considerations. The reduced tensile modulus is the only variable remaining. Thus flexure length will depend solely on this ratio. The table below gives this ratio for some cryogenic materials of interest:

Material	E	σ	$\sqrt{E/\sigma}$
	(GPa)	(MPa)	
AL (1100)	78.4	60	36.1
AL (5083)	78.4	170	21.5
AL (2014-T651)	78.4	550	11.9
SS (304)	224.0	1500	12.2
TI (6AL-4V ELI)	131.0	1650	8.9

A 6Al-4v ELI titanium flexure is 0.73 times the length of a type 304 stainless steel flexure and .25 times the length of an aluminum flexure. This illustrates the importance of selecting a material with a low reduced tensile modulus. The two materials which have the highest reduced tensile modulus are 6Al-4V ELI titanium and 5Al-2.55n ELI titanium. The latter material was used in the IRAS flexures (Ref. 5).

Additionally, the material selected for the flexures must have a high fracture toughness at cryogenic temperatures. Fracture toughness is the material property that identifies the materials' susceptibility to fracture.

Fused silica, which has excellent figure stability at cryogenic temperatures, is the candidate material for the primary mirror of the telescope. Interfacing fused silica with structural metals (such as titanium and aluminum) requires an innovative design because of the large differential thermal contraction that occurs when the system is cooled to cryogenic temperatures and the dynamic loading during launch.

For the 0.5-m double-arch primary mirror design, a mirror mounting system was developed at the University of Arizona that incorporates clamp and flexure assemblies (Ref. 9). Three clamp and parallel spring guide flexure assemblies are attached to the back of the mirror 120 degrees apart as shown in Figure 1. This design permits the supporting baseplate, which contracts more than the fused silica mirror during cryogenic cooldown, to transmit only acceptable intensities of bending moment and shear forces to the mirror. In addition, the flexure assemblies must be designed to ensure survivability of the system during the launch of the space shuttle. A representative random loading environment has been prescribed by the NASA SIRTF Technology Staff to define launch loading conditions. Excitation loadings have been determined in the form of power spectral densities (PSD) in the three mutually orthogonal directions. Assuming that cross-correlations do not exist between these loadings, the responses can be determined independently and superimposed when appropriate.

DESCRIPTION OF THE SELECTED MOUNT DESIGN

The selected design consists of a double arch primary mirror, a mirror socket, a two-bladed flexure, and a gimbal. For the 1.0-m. mirror an additional passive mechanism on the baseplate may be required to preload the flexure prior to cryogenic cool down.

The mirror socket assembly functions to transfer the system loads between the glass and socket support while maintaining an acceptable stress distribution within the glass which is of primary concern during launch. During launch, the mirror sockets' maximum loads occur in the tangential direction. Prior to and following launch the primary loads in the socket are in the radial direction and are caused by the cryogenic cool down.

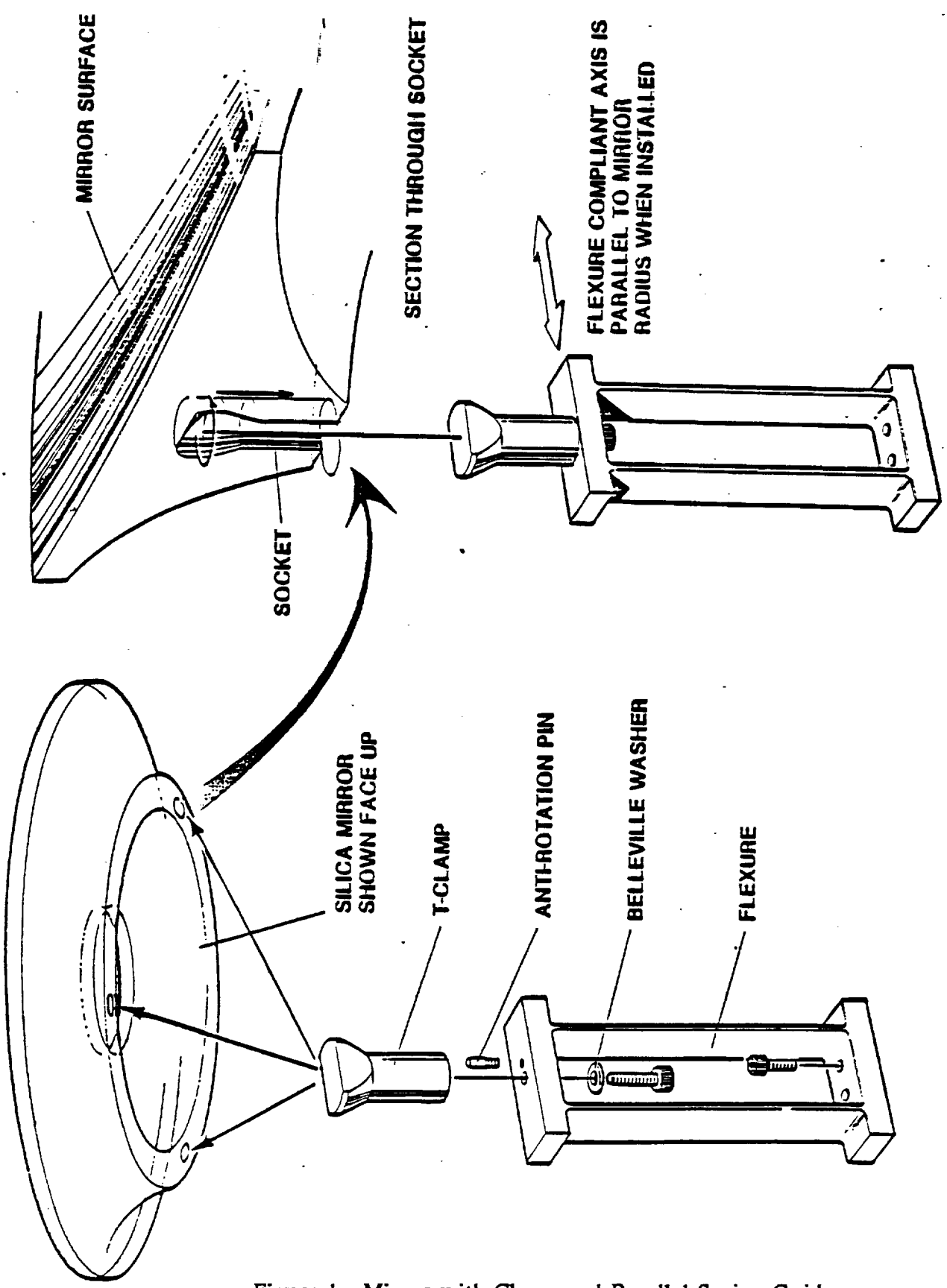

Figure 1. Mirror with Clamp and Parallel Spring Guide.

STRUCTURE MODELING FOR DYNAMIC ANALYSIS

A finite element model was constructed to evaluate the displacements and stresses in the 0.5-m primary mirror, the titanium flexures and gimbal, and the aluminum baseplate. A plot of the finite element mesh is shown in Figure 2. There are 925 nodes (3150 degrees of freedom), 384 solid hexahedron elements and 60 plate bending elements.

The four lowest free vibration frequencies and their mode shapes were determined and are shown in Figures 3 through 6. These mode shapes comprise:

1. translation in the y-direction
2. translation in the z-direction
3. twist about the x-axis which is the optical axis
4. translation in the x-direction

Because the relative stiffnesses of the mirror and the baseplate are significantly greater than the stiffness of the flexures for these displacement modes, the lower frequencies for the mirror-baseplate-flexure system are almost entirely dependent upon the stiffness of the flexures.

Execution of a dynamic analysis with a large model such as that shown in Figure 2 can be very time consuming and expensive. The time required of a single eigenvalue solution for this model is on the order of 900 CPU seconds on a CYBER 175. A simplified model (342 degrees of freedom) was therefore developed and used for the PSD loading analysis of the primary mirror support system. The mirror was replaced by rigid elements, and beam-bending elements were used to model the flexures. Execution time of an eigenvalue extraction using this simplified model was on the order of 30 CPU seconds.

A further simplified dynamic model of the support structure was developed wherein the translational flexibility of the system was completely described by bending and shear deformations of the flexures. Shown in the following analysis, the bending stiffness of each flexure is represented by two springs, corresponding to each of the

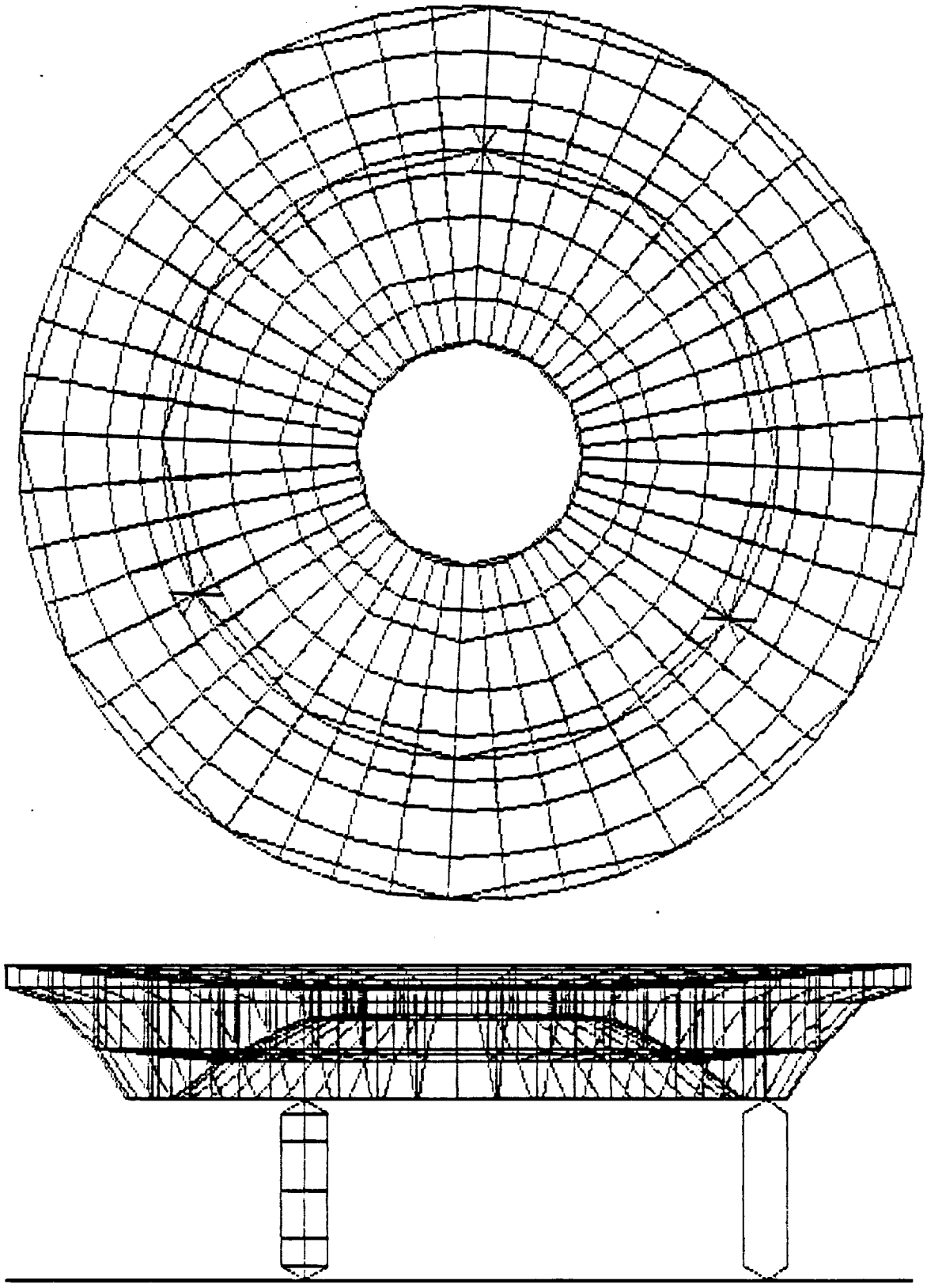

Figure 2. Finite Element Model

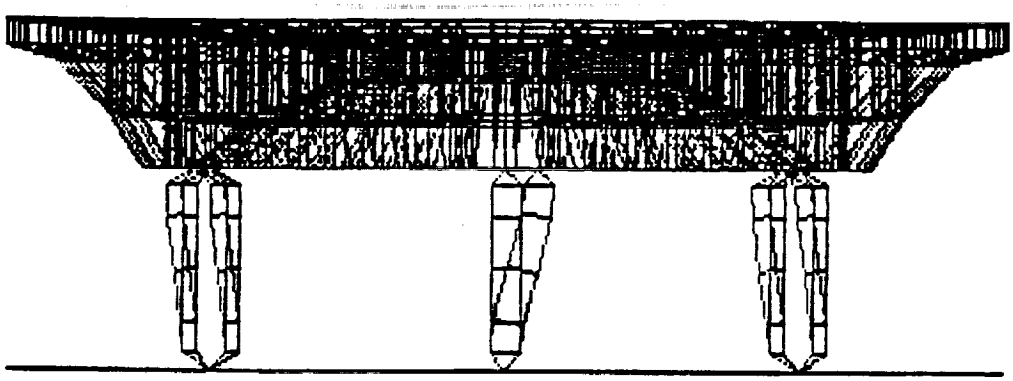

Figure 3. Mode Shape — Y Translation

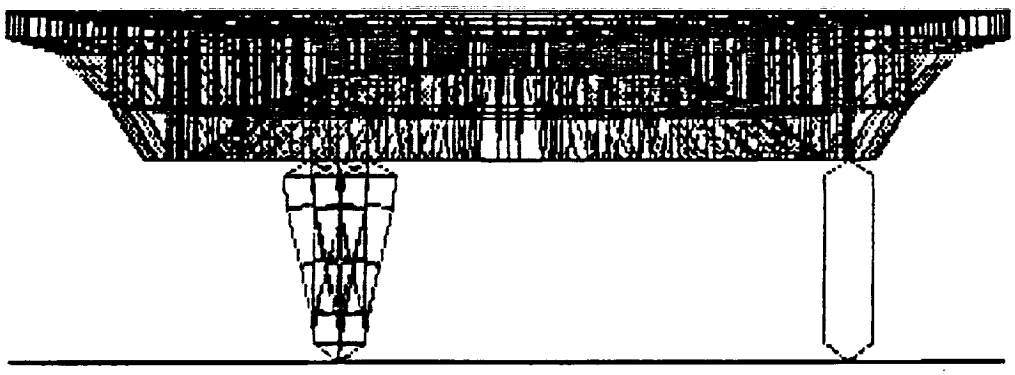

Figure 4. Mode Shape — Z Translation

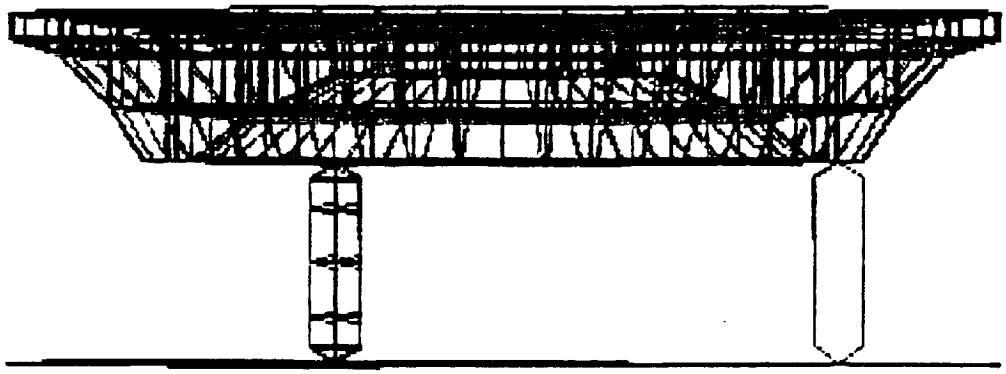

Figure 5. Mode Shape — Optical Axis Twist

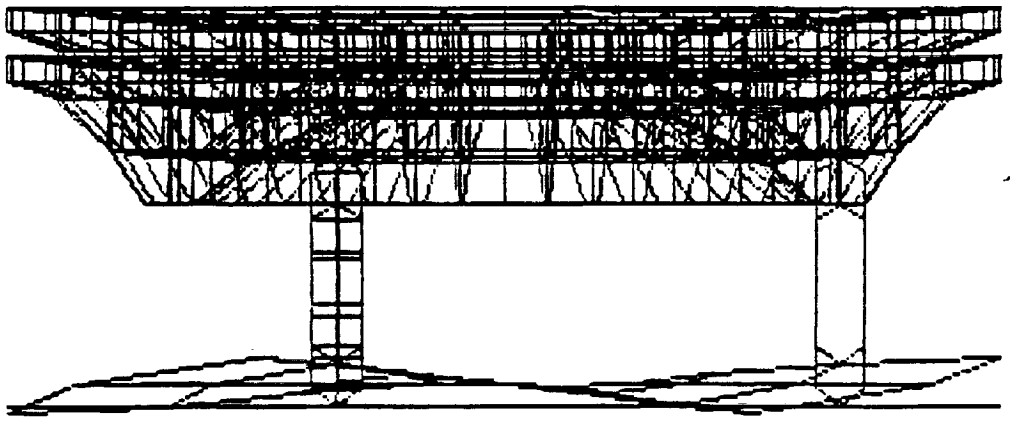

Figure 6. Mode Shape — Optical Axis Translation

principal displacements of the flexure assembly. That assembly resulted in a system such that a force applied in any direction results in a deflection co-linear with the applied force. That allowed the entire assembly to be modeled accurately as a single-degree-of-freedom system which translates in the y-z plane.

ANALYSIS OF THE SUPPORT SYSTEM FOR THE SIRTF PRIMARY MIRROR

The objective of this analysis is to provide assurance that the optical integrity of the SIRTF primary mirror will be maintained throughout its operational life. Two distinctly different loading conditions must be accommodated. Cryogenic cool down results in an elastic stress condition in which the surface deflections of the mirror must be small enough not to degrade its optical performance. Launch loads, on the other hand, cause stresses that must be small enough to avoid permanent deformation any place in the support system structure that could affect the mirror's preset optical alignment. As shown in Figure 7, the accommodation of these loading conditions can be divided into two categories: (1) Design a support system that will maintain the mirror's rms surface deflections during optical operation within those allocated in the wavefront error budget; (2) Design a support system that will maintain an internal stress distribution on each component so that throughout its life a factor of safety of at least three is kept on the materials' endurance limits.

The SIRTF Primary Mirror and Mount Wavefront Error Budget, provided by the NASA AMES SIRTF technology staff, is shown in Figure 8. During optical operations it allows a one μ-in. rms deflection on the surface of the primary mirror caused by the loading and associated deflections within the mirror's support system. In order to meet that requirement consideration has been given to manufacturing tolerances, the effects of cryogenic cool down, and the dimensional stability of the materials used. A listing of these design considerations is shown in Figure 9. The power spectral density (PSD) design curve for launch was also provided by the NASA AMES SIRTF technology staff and is shown in Figure 10. A constant $0.02g^2/Hz$ value extends to 250 Hz. A slope of -6.0 dB/octave is specified for frequencies greater than 250 Hz. An elastic stability

SIRTF PRIMARY MIRROR SUPPORT SYSTEM

OBJECTIVES OF ANALYSIS

I. DESIGN A SUPPORT SYSTEM THAT MAINTAINS THE RMS SURFACE DEFLECTIONS OF THE MIRROR DURING OPERATION WITHIN THOSE ALLOCATED IN THE ERROR BUDGET.

II. DESIGN A SUPPORT SYSTEM THAT HAS AN INTERNAL STRESS DISTRIBUTION SUCH THAT EACH COMPONENT HAS AT LEAST A FACTOR OF SAFETY OF THREE ON ITS MATERIAL'S ENDURANCE LIMIT.

Figure 7. Analysis Objectives

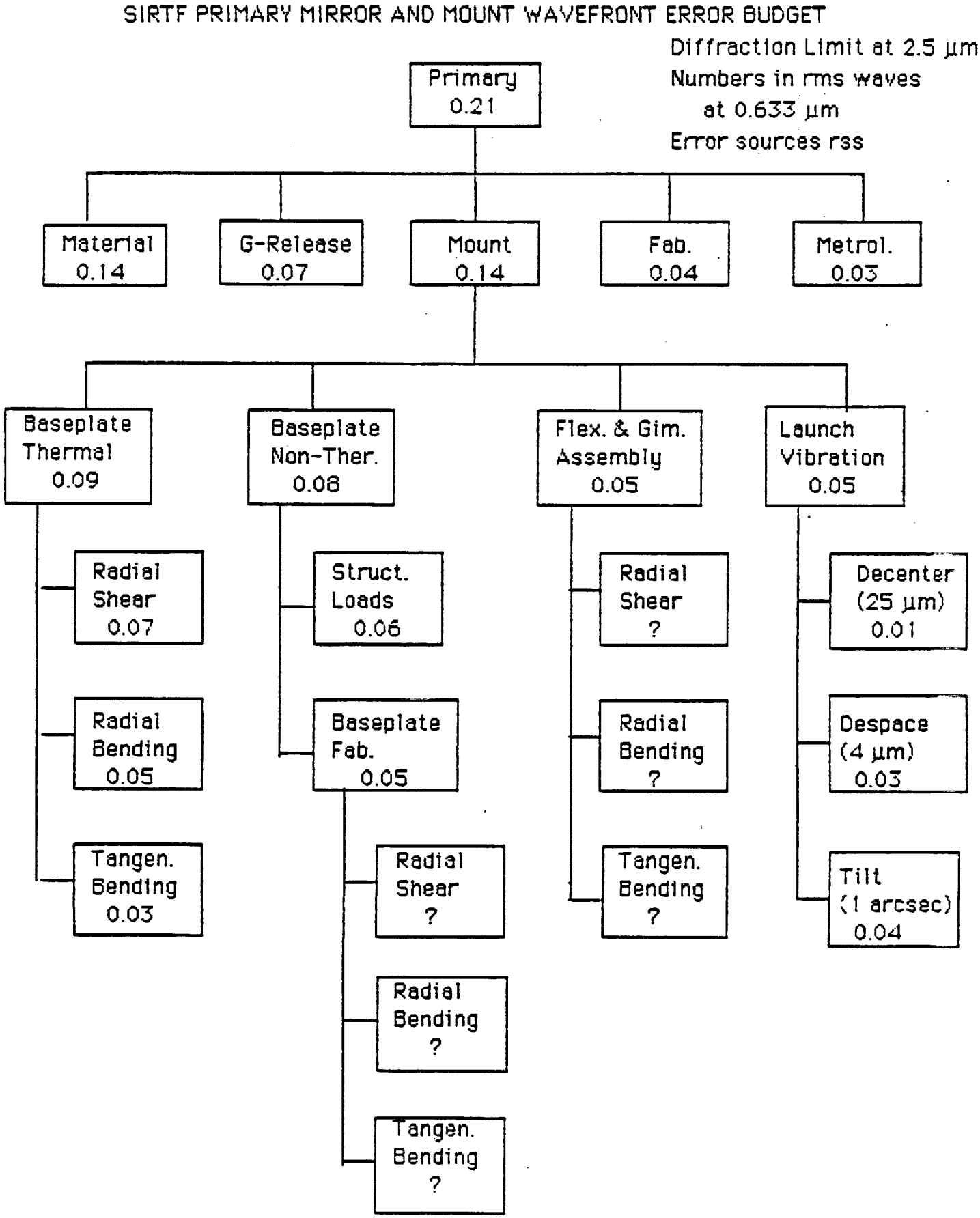

Figure 8. Wavefront Error Budget

SIRTF PRIMARY MIRROR

CONSIDERATIONS TO MEET OBJECTIVE I.

- CRYOGENIC COOLDOWN
- MANUFACTURING TOLERANCES
- MATERIAL'S DIMENSIONAL STABILITY

CONSIDERATIONS TO MEET OBJECTIVE II.

- LAUNCH POWER SPECTRAL DENSITY
- SYSTEM'S INTERNAL DAMPING
- ELASTIC STABILITY (BUCKLING)

Figure 9. Design Considerations

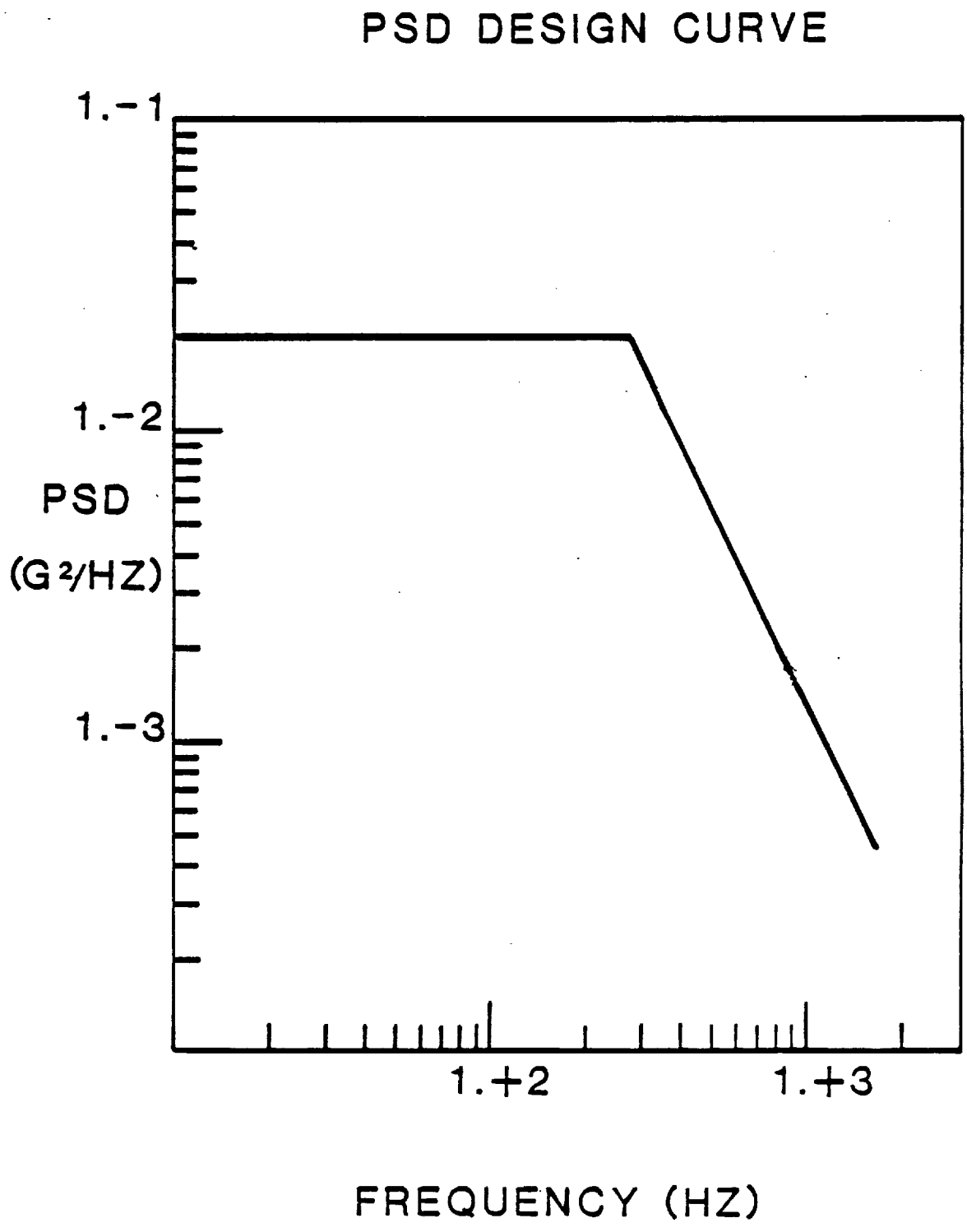

Figure 10. PSD Design Curve

(buckling) analysis was performed to determine the critical loads and buckling mode shapes of the mirror support system. The dynamic loads were then compared to the buckling loads to ensure that the system remained stable during launch. At that time the surface deflections of the primary mirror are allowed to exceed those specified within the wavefront error budget because the optical systems will not be in operation. The system's internal loads are therefore allowed to be higher during launch than during optical operation. The upper limit on those loads is established by the requirement that no permanent set can be permitted in any single part that could degrade the optical performance. This resulted in the design objective of maintaining at least a safety factory of three on the materials' endurance limits. It also makes any buckling unacceptable.

The method of evaluating the optical effects caused by mechanical and thermal loads is shown in Figure 11. First, a structural model of the mirror and support system is prepared for either the finite element program, SAP IV or NASTRAN. Modeling for the finite element program involves describing the geometry of the structure, identifying specific properties of the materials, and specifiying the loading to be input into the program. Upon execution of the finite element program, an output file is created that contains both the input data and the structural defelctions of the mirror surface. That output file becomes a portion of the input file to the program FRINGE. FRINGE has been modified to accept structural deflections as input data and to internally translate these deflections to units of wavelengths. The output includes rms deflections, contour plots, spot diagrams, encircled energy plots and Zernickie polynomial coefficients. This procedure was used to establish an upper limit for the loads on the SIRTF primary mirror that would not exceed the rms deflections specified in the wave front error budget. The study consisted of applying unit shear loads and bending moments in the horizontal plane of the mirror that contains its center of gravity. These shear loads and bending moments were located at each of the three socket locations and aligned in the directions that correspond to the socket loading on the mirror during cryogenic cool

Figure 11. Analysis Flow Chart

down.

From the results of this study, shown in Figure 12, it was concluded that a shear load contained within the plane of the mirror's center of gravity has a negligible effect on the mirror's optical performance. It was also concluded that a unit bending moment at each of the socket locations results in an rms deflection of the mirror's surface of 32.91 nanoinches/inch pound. In dividing the allowable rms deflection of 1 μin. by this influence coefficient, the allowable bending moment at each of the three sockets is 30.4 inch pounds.

The requirements for the primary mirror support system result in an interaction of requirements on each of the subcomponents. These interactions, summarized in Figure 13, provide constraints such that design space boundaries are formed. First, the support system must have a soft radial translational stiffness to survive the cryogenic cool down without distorting the surface of the mirror. Because the coefficient of thermal expansion of the glass is very small compared to that of the aluminum baseplate, the differential radial contraction of the aluminum baseplate represents the radial deflection that must be accommodated by the support system. This results in a shear and bending moment applied to the mirror that will remain throughout the lifetime of SIRTF. As previously discussed, the shear load effects are small compared to those of the bending moment. To minimize the bending moment, the radial translational stiffness of the support system must be as low as possible. Alternatively, the support system must have a large translational stiffness between the baseplate and mirror in at least one direction in order to survive the launch loads. The reason for this will be discussed in detail later in this report and it will be shown that although the stiff direction could be in either the radial or tangential direction, or both, the first requirement for low stiffness in the radial translational direction makes it necessary to design a stiff support system in the tangential direction only. A third requirement is that the support system remains elastically stable and not buckle. This is consistent with the second requirement discussed above but is in conflict with the first. The very dimension that makes a

SIRTF PRIMARY MIRROR

ALLOWABLE LOADS AT PLANE OF MIRROR'S CG DURING OPTICAL OPERATION OF SIRTF

- ERROR BUDGET ALLOCATION
  - CURRENTLY $\leq 1 \times 10^{-6}$ IN RMS
- INFLUENCE COEFFICIENT FROM NASTRAN/FRINGE RUNS
  - IN CG PLANE OF MIRROR, SHEAR HAS NEGLIGIBLE INFLUENCE ON SURFACE DISTORTION
  - IN CG PLANE OF MIRROR MOMENTS:
    - .5 METER
      $RMS_{co} = 3.291 \times 10^{-8} \frac{IN}{IN\text{-}lb}$
    - 1.0 METER
      $RMS_{co} = 1.338 \times 10^{-8} \frac{IN}{IN\text{-}lb}$
- MOMENT ALLOWED
  - .5 METER
    $M_{ALLOW} = 30.4$ IN-lb
  - 1.0 METER
    $M_{ALLOW} = 74.7$ IN-lb

Figure 12. Allowable Loads During Optical Operation

SIRTF PRIMARY MIRROR

INTERACTION OF SYSTEM REQUIREMENTS FOR THE SUPPORT SYSTEM

- THE SYSTEM MUST HAVE A SOFT RADIAL TRANSLATIONAL STIFFNESS TO SURVIVE CRYOGENIC COOLDOWN.

- THE SYSTEM MUST HAVE A HARD TRANSLATIONAL STIFFNESS (EITHER RADIAL OR TANGENTIAL OR BOTH) TO SURVIVE LAUNCH.

- THE SYSTEM MUST HAVE A HARD TRANSLATIONAL STIFFNESS TO PREVENT BUCKLING.

- THE SYSTEM MUST HAVE SOFT RADIAL AND TANGENTIAL ROTATIONAL STIFFNESS TO ACCOMODATE MANUFACTURING TOLERANCES AND MATERIAL DIMENSIONAL INSTABILITIES.

Figure 13. Interaction of System Requirements

component translationally low in stiffness makes it susceptible to buckling. The fourth requirement is that the support system have low radial and tangential rotational stiffnesses to accommodate manufacturing tolerances and dimensional instabilities of the materials. The manufacturing tolerances of concern include the parallelism of the top and bottom of the support system itself where it interfaces with the mirror and baseplate. Also of concern is the relative parallelism of the regions on the mirror and baseplate where the support structure is attached. Any lack of parallelism of these surfaces will cause a local rotation, without a corresponding translation, of the support system. In the stiff direction of the support system, it is apparent that a large bending moment might well be transmitted to the mirror for a very small angle associated with lack of parallelism. As will be shown later, the flexure contained in the support system, when rotated in this manner in its soft direction, will also transmit a significant bending moment to the mirror for a very small angle associated with a lack of parallelism.

The primary mirror mount support selected for SIRTF is shown in Figure 14. Three sub-assemblies make up this support system: the gimbal, which mounts directly to the baseplate; the mirror socket assembly, which mounts directly to the mirror; and the flexure, which connects these two. The primary purpose of this support system is to accommodate the relative displacements of the mirror and baseplate during cryogenic cool down. The flexure was designed to perform that function. Once the flexure was sized for this purpose, it was modified to accommodate the launch loads without buckling or being overstressed. When these conditions were met, it was not possible to meet the requirement for local rotations caused by manufacturing out-of-plane tolerances. A gimbal support provides a low torsional stiffness at the base of the flexure that allows substantial out-of-parallelism of mating surfaces that may result during fabrication. If the rotational mismatches can be accommodated by the gimbal, the mount can be attached to both the mirror and the baseplate with a predetermined and acceptable bending moment being transmitted to the mirror. The gimbal also can

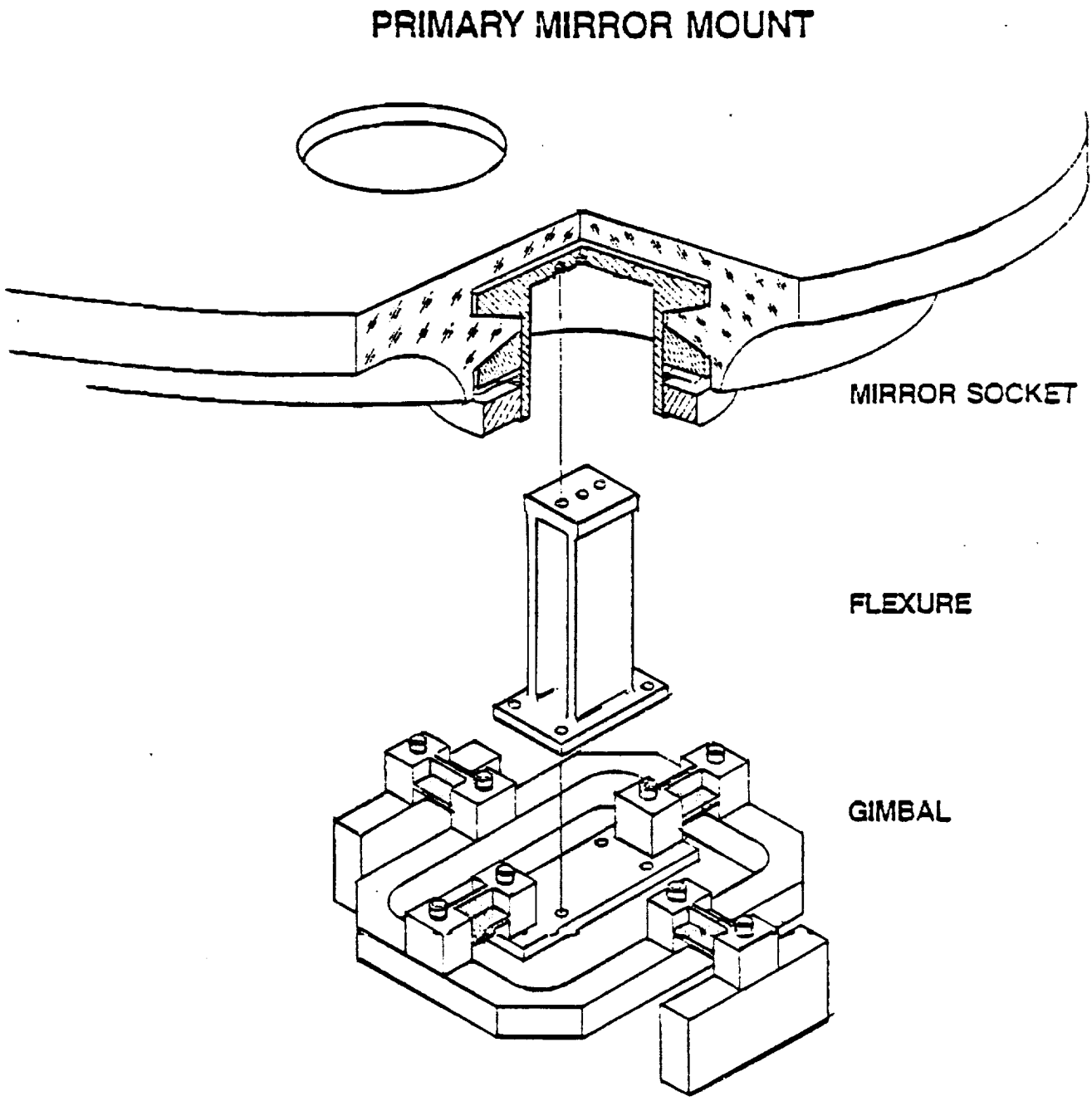

Figure 14. Primary Mirror Mount

accommodate material dimensional instabilities that may occur. A further attribute of the gimbal is that the radial translational stiffness of the support system becomes completely decoupled tangential translational stiffness.

The use of a parallel spring guide to give a low stiffness in the radial translational direction and provide for a stiff spring in the tangential translational direction has been incorporated into the mirror support design. The flexure loaded in the stiff direction is shown in Figure 15, and the flexure loaded in the soft direction is shown in Figure 16. The flexure loading shown in Figure 16 represents the loading during cryogenic cool down. Descriptive sketches which show the internal load distribution during cool down are given in Figure 17. Sketch (a) shows the center post connecting the gimbal at point P where the gimbal shear load, V, acts with essentially zero moment because of the soft torsional spring stiffness of the gimbal. The distance from the point, P, to the plane of the mirror's center of gravity is C; thus, the shear load, V, causes a moment in the plane of the mirror equal to V times C. Sketch (b) shows the flexure blade in the loaded condition where the baseplate has moved radially inward an amount labeled delta. In this configuration an ideal parallel spring guide would translate in such a way that the parallel surfaces at the end of the flexure would remain parallel. However, as shown in sketch (c) of Figure 17, the internal distribution of load can be broken into two parts. First, the distribution for the shear, V, is independent of the post height. Further, the axial load in the legs of the flexure form a couple that can be calculated from equilibrium of the lower surface of the flexure. The second part of the internal distribution of loads is just the moment which results when transferring the shear to the base of the flexure. That moment is reacted by forces in the legs which form a couple equal to V times a. It is seen that when the post height, a, is half the flexure length, these couples cancel each other resulting in zero axial load in the flexure legs, and the flexure acts as a true parallel spring guide. For the SIRTF mirror support structure, it was not possible to make the post height half of the flexure length. With the incorporation of the gimbal into the system, however, the small rotation that results

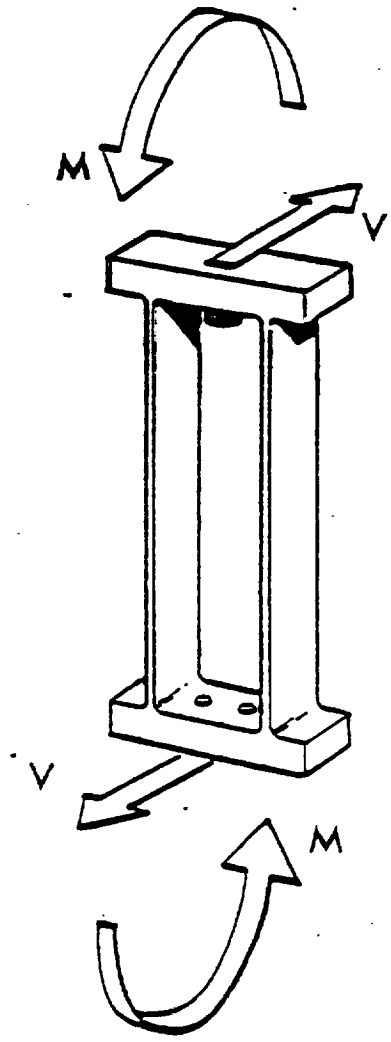

Figure 15. Flexure — Loaded in Stiff Direction

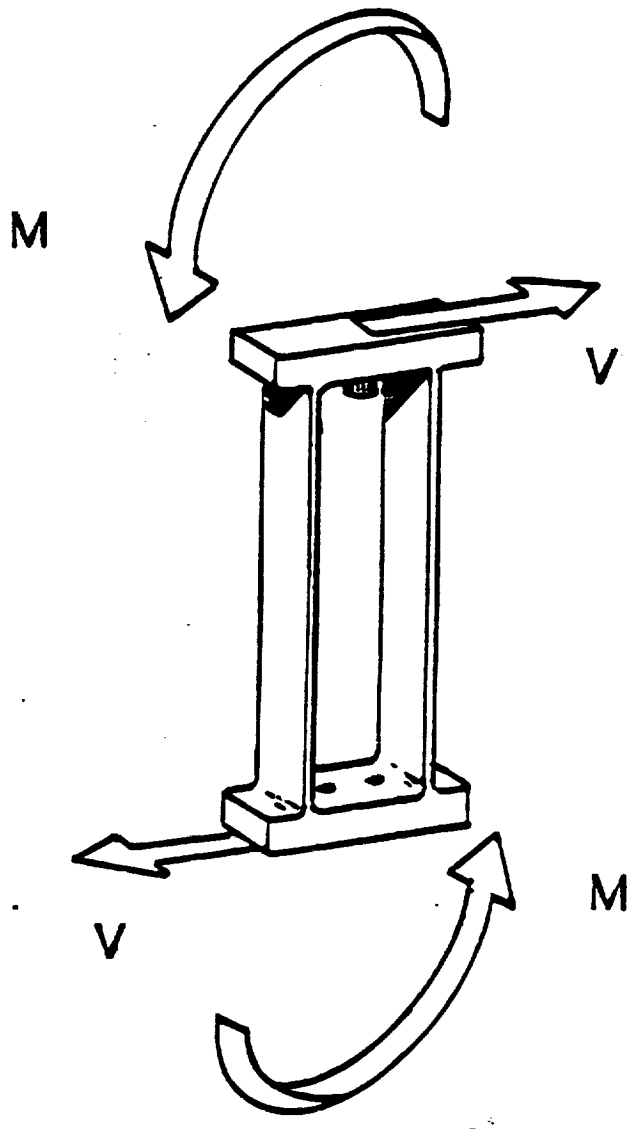

Figure 16. Flexure — Loaded in Soft Direction

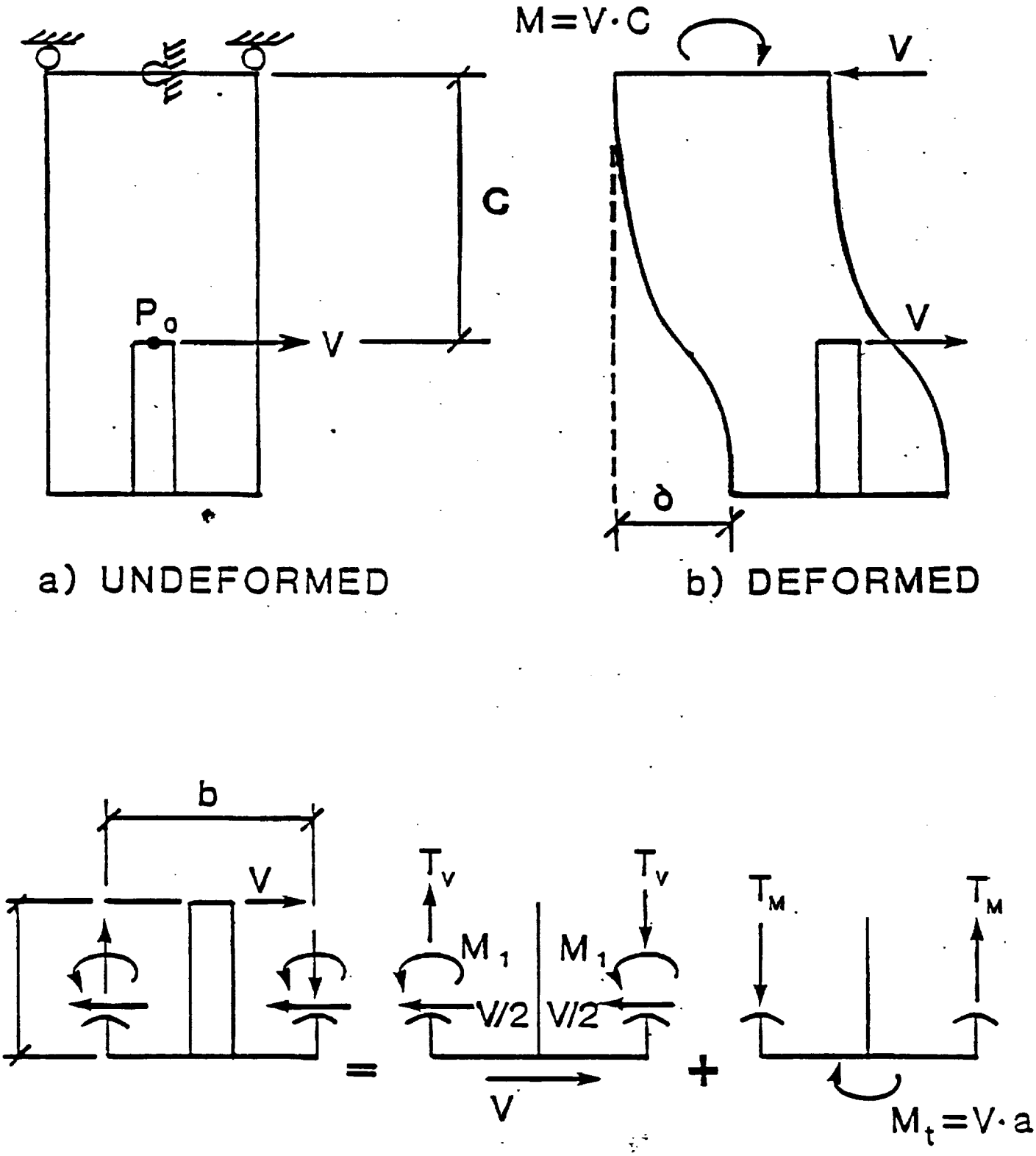

Figure 17. Flexure — Internal Load Distribution

is accommodated without any significant additional bending moment being applied to the mirror.

The three-point support system chosen for the SIRTF primary mirror is kinematically stable and statically determinate so that it is difficult to lock in unidentified residual loads. Each of the three support assemblies is shown in Figure 14. A force diagram of that support system is shown in Figure 18. Each reaction represents the equivalent spring force of the Figure 14 assembly so that a system of equations for the reaction loads can be established. Because of symmetry, effective spring constants can be determined as shown in Figure 19. These constants, Ka and Kb, each include the structural properties of both the flexure and the gimbal. If a force is applied to this system in an arbitrary direction, theta, as shown in Figure 18, the deflection that results is colinear with this force. Furthermore, the resultant stiffness is independent of theta. Summarizing, the displacement is always colinear with the force, and the stiffness, which is the same in all directions, is equal to 1.5 (Ka + Kb).

This linearly-elastic system can be treated as a single-degree-of-freedom system. The system stiffness relationships are shown in Figure 20. For the SIRTF 0.5-m mirror support system, Kb is approximately a factor of 100 times that of Ka so that Ka can be ignored, thereby simplifying the equations. However, Ka is included in the NASTRAN model and computations. The simplified analyses and the computer analyses typically agree to within five percent of each other.

Flexure blade parameters that must be included when calculating the values for Ka and Kb are the bending and shear stiffnesses. These two stiffnesses add as two springs in series. Gimbal blade parameters which must be included when calculating the values for Ka and Kb are also the bending and shear stiffnesses. These also add as two springs in series. The system parameters for Ka and Kb are summarized in Figure 21. When the soft spring, Ka, is ignored, the resulting equations for the single-degree-of-freedom system are as shown in Figure 22. Kss becomes Kb and the system's spring rate is 1.5 times Kss. The equation shown includes the effects of the post height; the

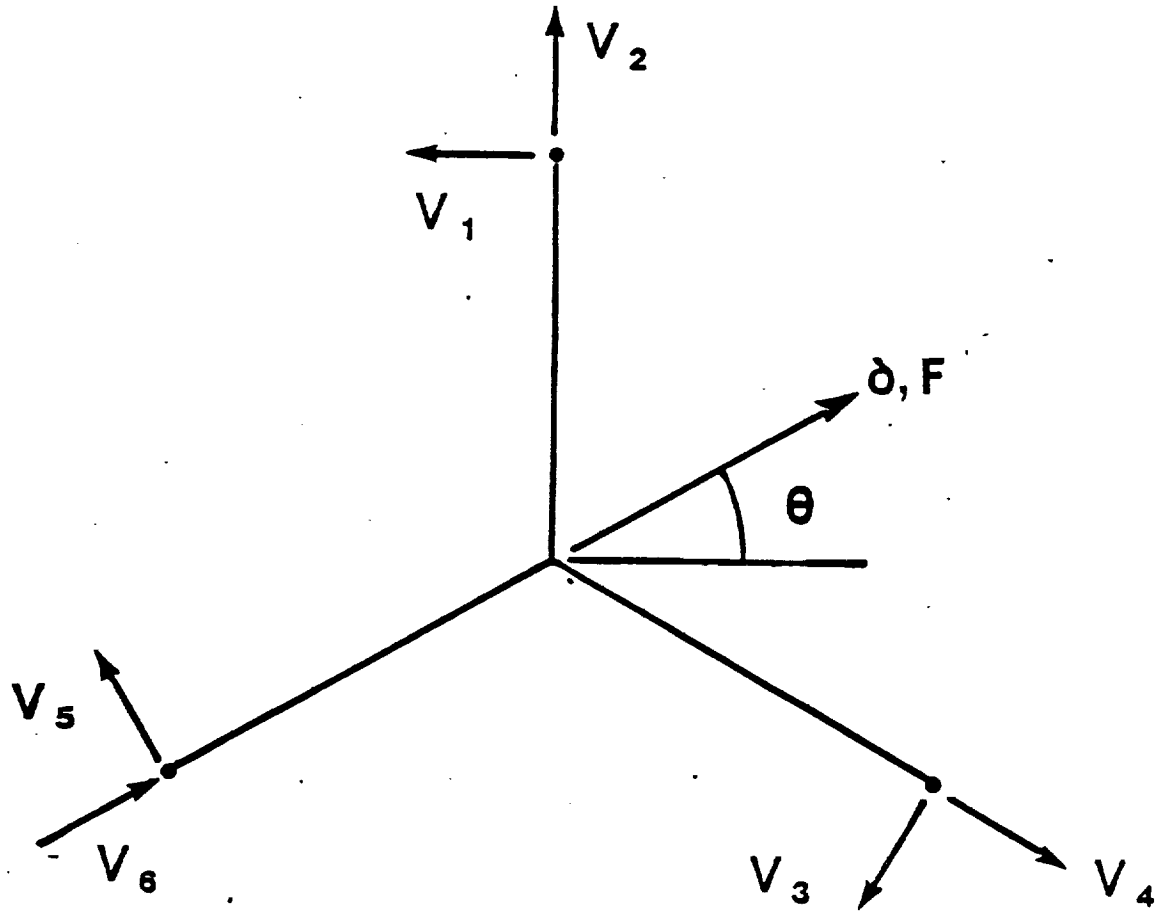

Figure 18. Model of System Force Balance

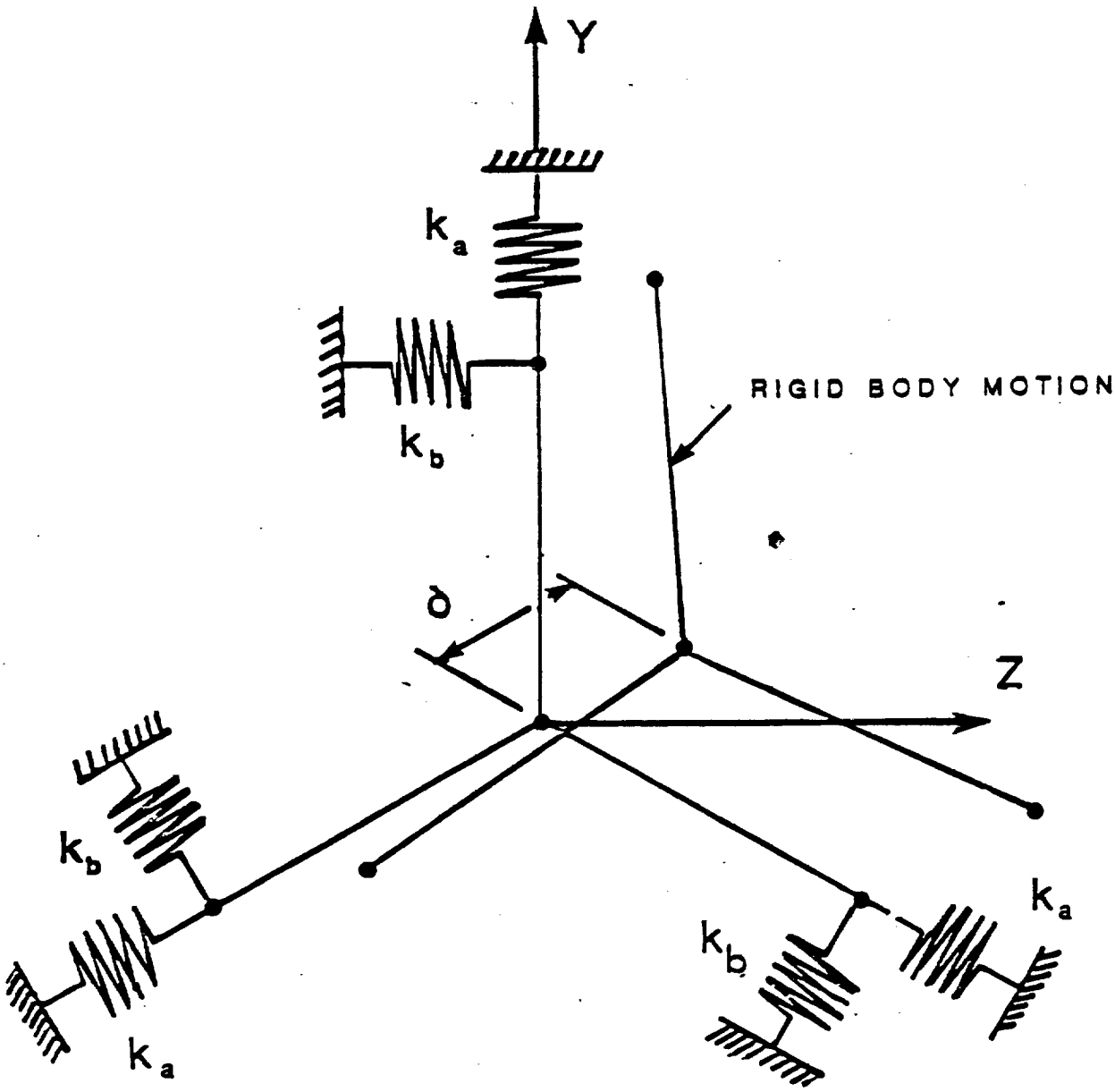

Figure 19. An Equivalent Spring Support System

SIRTF PRIMARY MIRROR

FOR A SUPPORT SYSTEM RADIALLY SYMMETRIC AT 120 DEGREES

$$K_{SYS} = 1.5\ (K_a + K_b)$$

WHERE:

K_{SYS} = SYSTEM STIFFNESS

K_a = RADIAL TRANSLATIONAL STIFFNESS

K_b = TANGENTIAL TRANSLATIONAL STIFFNESS

$K_a << K_b$

Figure 20. An Equivalent Single-Degree-of-Freedom Spring Support System

SIRTF PRIMARY MIRROR

$$K_{sys} = 1.5\,(K_a + K_b)$$

SUB SYSTEM PARAMETERS IN K_a AND K_b

- FLEXURE BLADE
  - BENDING STIFFNESS
  - SHEAR STIFFNESS
- GIMBAL BLADE
  - BENDING STIFFNESS
  - SHEAR STIFFNESS
  - TORSIONAL STIFFNESS

Figure 21. Subsystem Parameters Contained in K_a and K_b

SYSTEM STIFFNESS PARAMETERS

$$K_{SYSTEM} = 1.5\, K_{ss}$$

$$\frac{1}{K_{ss}} = \left[\left(1 + \frac{\left(\frac{3d}{2\ell}\right)}{\left(1 + \frac{K_r \ell}{4EI}\right)} \right) \left(\frac{\ell^3}{12EI} \right) \left(\frac{1 + \frac{K_r \ell}{4EI} + \frac{3d}{2\ell}}{1 + \frac{K_r \ell}{4EI} - \frac{3}{4}} \right) + \frac{\left(d^2 \frac{\ell}{4EI} \right)}{\left(1 + \frac{K_r \ell}{4EI} \right)} + \frac{1}{K_t} + \frac{1}{\frac{2AG}{\ell}} \right]$$

WHERE :

K_{SYSTEM} = SYSTEM STIFFNESS

d = POST HEIGHT

ℓ, I, A = FLEXURE PARAMETERS

K_r, K_t = GIMBAL PARAMETERS

Figure 22. System Stiffness Parameters

flexure blade parameters of length, area, and moment of inertia; and the gimbal torsional stiffness and translational stiffness which include the effects of shear and bending deflections of the gimbal blades.

A parametric design study is possible by using the equations summarized in Figure 23. These equations include the system stiffness equation and, in addition, the rms deflection based on the PSD design curve and the system damping coefficient. For low system damping, as is the case for the SIRTF system, the undamped natural frequency is essentially equal to the natural frequency of the system. The third equation in Figure 23 gives the rms deflection for a white noise excitation of a single-degree-of-freedom system with a damping ratio, rho, and a natural frequency, fn. A parametric analysis was performed using these three equations as follows: First, the system parameters are selected which can be systematically assessed through a DO loop in a Fortran computer program. For each set of parameters selected, the system's stiffness can be calculated. Combining the system's stiffness with the mass of the mirror, the system's natural frequency can then be calculated. Combining the system's natural frequency with the damping ratio of 0.004, which was measured in recent tests at the NASA AMES Research Center, and the PSD curves, which were furnished by the NASA AMES SIRTF technology staff, the rms deflection of the mirror can then be calculated. The rms deflection thus determined is the result of a single axis PSD. However, the system design requirement is that the same PSD curve can activate the system on any two mutually orthogonal horizontal planes as well as along the optical axis. That design requirement is conservatively accommodated by assuming that the two horizontal excitations are equal in magnitude and in phase. The much larger vertical stiffness of the system essentially decouples the vertical response from the lateral responses. Adding the two horizontal responses as described above results in the fourth equation of Figure 23. It simply states that the resultant displacement is 1.414 times a single axis PSD response which is the vector sum of the two. Although the single-degree-of-freedom stiffness is not a function of the angle of the applied loads, the

SIRTF PRIMARY MIRROR DESIGN EQUATIONS

$$K = 1.5(K_a + K_{ss}) \qquad K_a << K_{ss}$$

$$fn = \frac{1}{2\pi}\sqrt{\frac{K}{M}}$$

$$\delta_{RMS} = \left(\frac{PSD}{(1984)(\rho)(fn^3)}\right)^{\frac{1}{2}}$$

$$\delta_{SYS} = 1.414\,(\delta_{RMS})$$

WHERE:

K = SYSTEM STIFFNESS

K = FLEXURE ASSEMBLY STIFFNESS-SOFT

K = FLEXURE ASSEMBLY STIFFNESS-HARD

M = MASS OF MIRROR

fn = SYSTEM UNDAMPED NATURAL FREQUENCY

PSD = VALUE OF PSD AT fn

ρ = SYSTEM DAMPING RATIO

δ_{RMS} = SYSTEM RMS DEFLECTION DUE TO A SINGLE PSD INPUT

δ_{SYS} = SYSTEM RMS DEFLECTION DUE TO TWO MUTUALLY ORTHOGONOL PSD INPUTS

Figure 23. Primary Mirror Socket Loads

internal load distribution of the support system is very much a function of the orientation of the applied loads. The internal load distribution was determined as a function of the angle of the applied load. By differentiating the load-displacement equation with respect to that angle and setting the resulting expression to zero, the angle causing the maximum internal load distribution on a given support assembly was found. It was found that the resulting force vector is exactly aligned with one of the support assemblies. Maximum stresses can therefore be calculated on a single-support assembly by imposing a deflection on that assembly in its stiff or tangential direction equal to 1.414 times the system's rms deflection caused by a single axis PSD.

From the results of the analysis described above, the flexure blade width, blade length, and blade thickness can be chosen such that the maximum flexure assembly stress is 43,000 PSI. The analysis can then be summarized on the flexure blade width, length and thickness (B-L-T) curve as shown in Figure 24. Design constraints can then be imposed on that curve to identify the available design space. For instance, the geometric constraint that any flexure less than two inches long will not be able to be installed is identified on the curve. In addition, the constraint that any flexure wider than one inch will require a socket that is too large for the 0.5-m mirror is also identified on the curve. In order to minimize the bending moment going into the mirror during cryogenic cool down, the minimum value of blade thickness can be selected from the remaining design space. The resulting design configuration was selected by rounding the calculated dimensions to those normally considered in manufacturing. Specifically, the flexure blade dimensions selected are those shown in Figure 25. System loads, stresses and factors of safety are summarized for the 0.5-m primary mirror in Figure 25. Conditions are shown with and without a gimbal. The rounding of dimensions to manufacturing norms is reflected in the reduced factors of safety of 2.5 and 2.7 on the material's endurance limit as shown in Figure 25. One of the objectives of the design was to maintain a minimum factor of safety of three on the material's endurance limit. Although this exception was determined to be acceptable

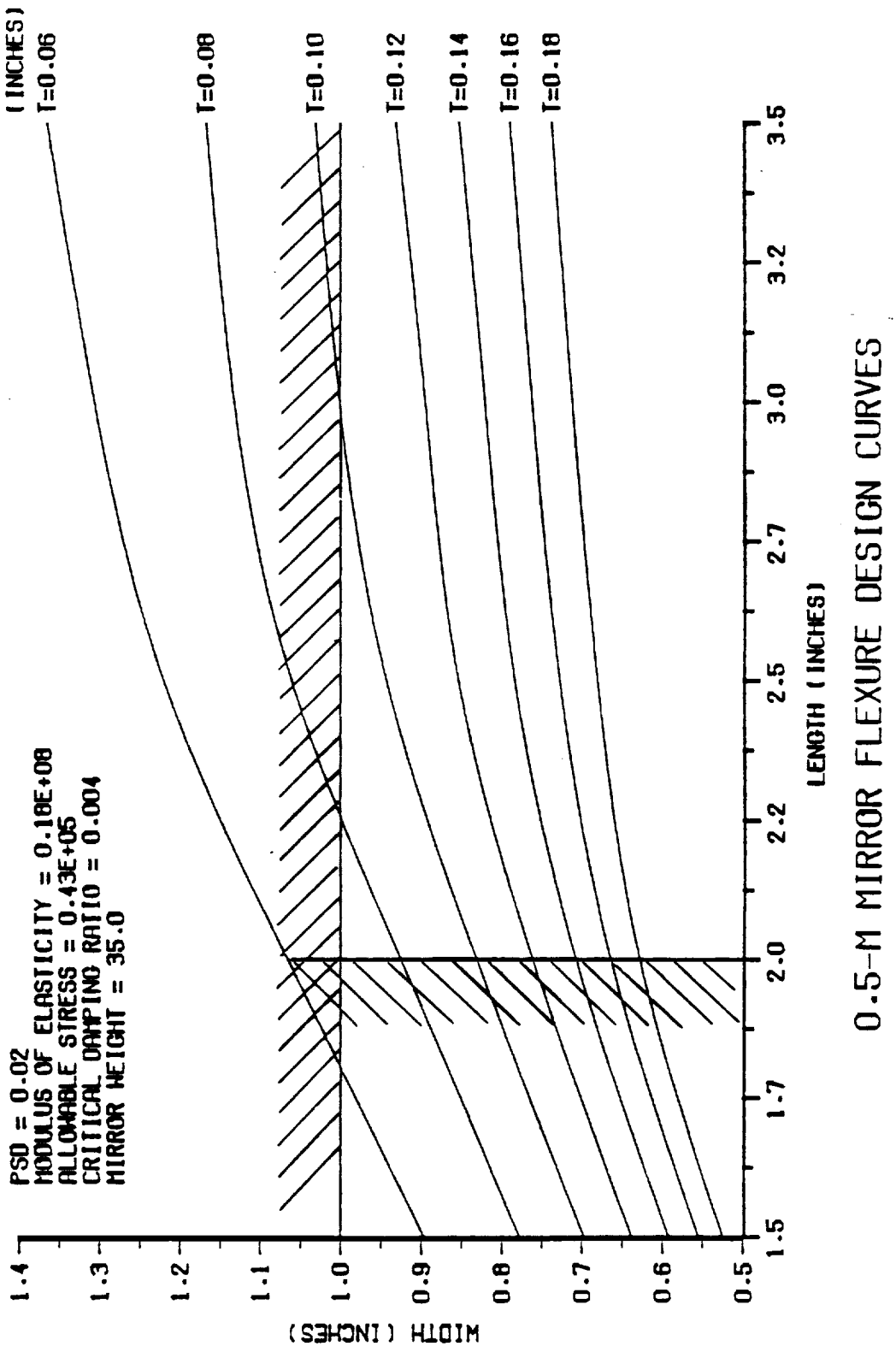

Figure 24. B-L-T Curves Illustrating the Available Design Space

.5 METER PRIMARY MIRROR

SUMMARY

BLADE SIZE : 2" LONG
1" WIDE
.060" THICK

PARAMETER	W/O GIMBAL	W/GIMBAL
SYSTEM K (lb/in)	245,600	156,900
fn (Hz)	262	209
δ RMS (in)	4.36×10^{-3}	6.41×10^{-3}
V_{CR} (lb) NASTRAN BUCKLING	8,970	7,080
V_{SYSTEM} (lb)	1,510	1,400
V_{MAX} SINGLE SOCKET (lb)	975	900
V_{CRYO} SINGLE SOCKET (lb)	31.4	31.4
M_{CRYO} (in-lb)	51.8	51.8
M_{ALLOW} (in-lb) 1×10^{-6} in-RMS	30.4	30.4
σ_{MAX} (PSI) TWO ORTHOGANAL PSD	50,400	46,700
σ_{ALLOW} (PSI) ENDURANCE LIMIT	130,000	130,000
σ_{ALLOW} (PSI) YIELD	280,000	280,000
FS YIELD	5.5	8.0
FS ENDURANCE LIMIT	2.5	2.7

Figure 25. 0.5-M Design Summary

for the 0.5-meter mirror, the factor of safety of three on the material's endurance limit will be maintained on the 1.0-m mirror.

Socket loads can be calculated directly from the equations included in the above analysis. Tangential shear loads are taken directly from that analysis. Moments and their mode of reaction at the socket are established from the shear loads and the specific geometry of the socket design. Equations summarizing the procedure are shown in Figure 26. Vertical loading obtained from the PSD design curve has been included in that analysis also. Vertical loads are small compared to the lateral loads, however. For that reason, a parametric analysis can be developed using the parameters contained in the equation in Figure 22. When that study is accomplished, curves such as those shown in Figures 27 and 29 can be developed to see the effects of the flexure post height, the gimbal's torsional stiffness, and the gimbal's lateral stiffness.

Successfully accommodating cryogenic cool down is the prime design requirement of the SIRTF primary mirror support system. This requirement has been satisfied by a gimballed flexure for the 0.5-m mirror. Early indications are that such a system might not work for the 1.0-m mirror; therefore, two options are being investigated specifically for it. Those options could certainly be incorporated into the 0.5-m mirror support system, as well, should that be desired. Option one is a gimbal modification that replaces the cruciforms in the radial direction with rectangular flexures. That is the decoupling capability of the gimbal that was discussed earlier. The results of that study will be reported later. Option two is the preloading device shown in Figure 30. It allows the baseplate to be adjusted prior to the support system assembly such that the baseplate can then preload each of the three support system assemblies in the radial direction. Cryogenic cool down then shrinks the baseplate and relieves the prestress in the support system, thereby relieving the bending moments and associated deflections in the mirror.

For the candidate configurations being considered for the 1.0-m mirror, the analytic procedure developed herein for the 0.5-m mirror can be used to determine loads and

SIRTF PRIMARY MIRROR DESIGN EQUATIONS

MAXIMUM LATERAL SOCKET LOADS

TANGENTIAL

$$F_T = K_{ss}\,\delta_{SYS}$$

$$M_T = C \times F_T$$

RADIAL

$$F_R = K_a\,\delta_{CRYO}$$

$$M_R = C \times F_R$$

WHERE:

F_T = TANGENTIAL SHEAR FORCE

M_T = MOMENT AT MIRROR CG DUE TO F_T

F_R = RADIAL SHEAR FORCE

M_R = MOMENT AT MIRROR CG DUE TO F_R

δ_{SYS} = MAXIMUM RMS SYSTEM DISPLACEMENT

δ_{CRYO} = RADIAL DISPLACEMENT OF BASE PLATE DUE TO CRYOGENIC COOLDOWN

C = DISTANCE FROM GIMBAL PLANE TO MIRROR CG PLANE

Figure 26. System Design Equations

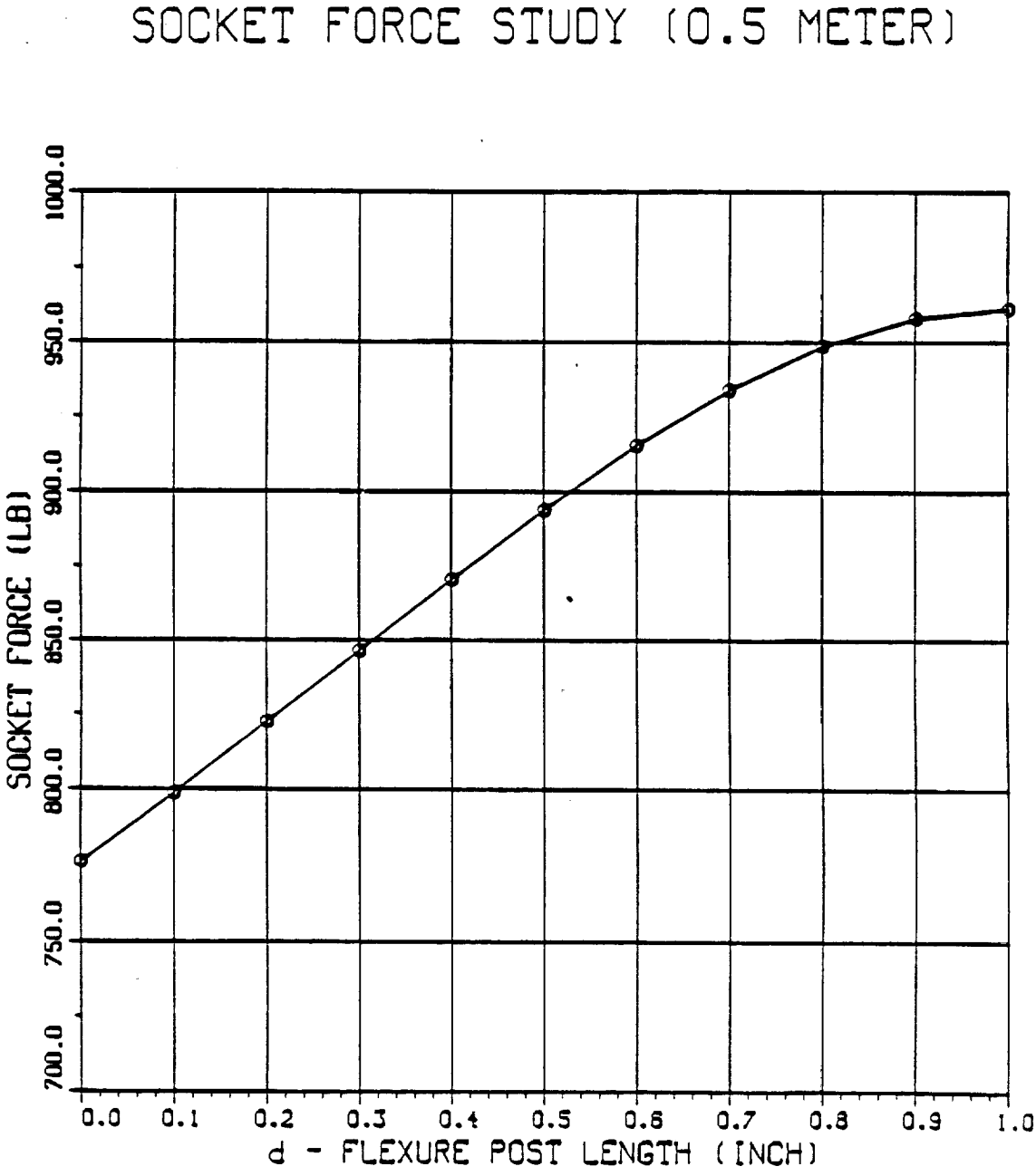

Figure 27. Socket Force Vs. Flexure Post Length

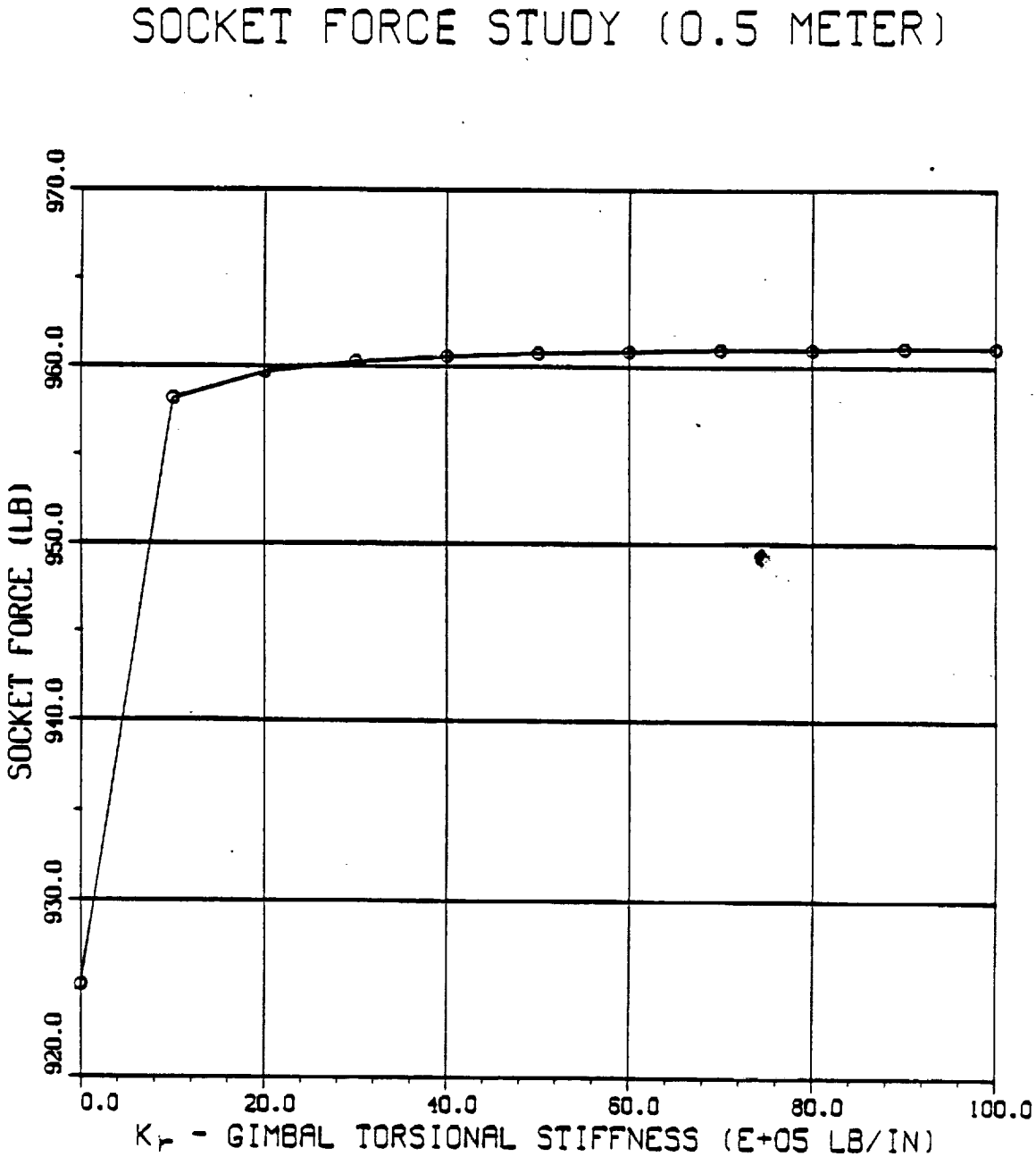

Figure 28. Socket Force Vs. Gimbal Torsional Stiffness

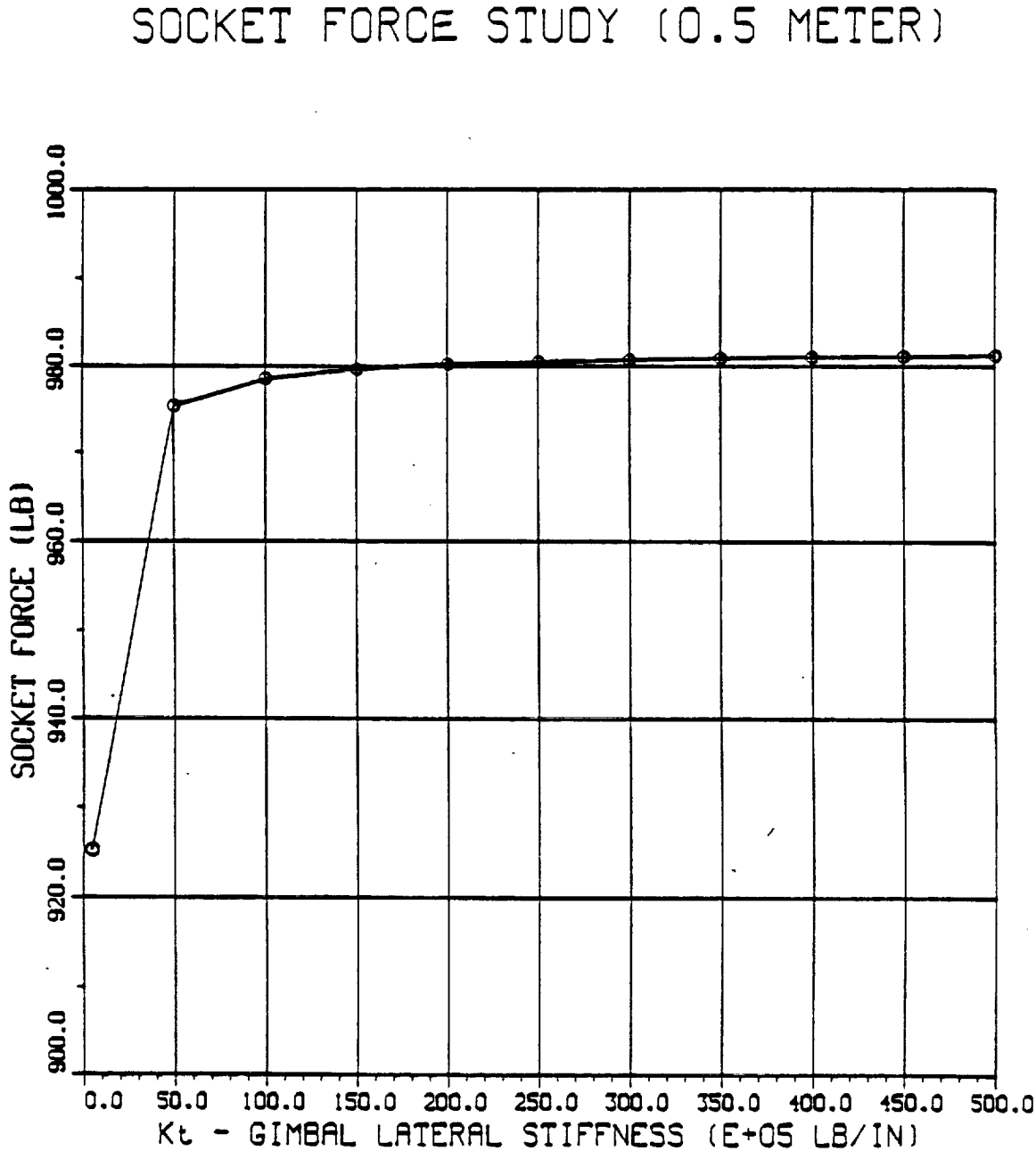

Figure 29. Socket Force Vs. Gimbal Lateral Stiffness

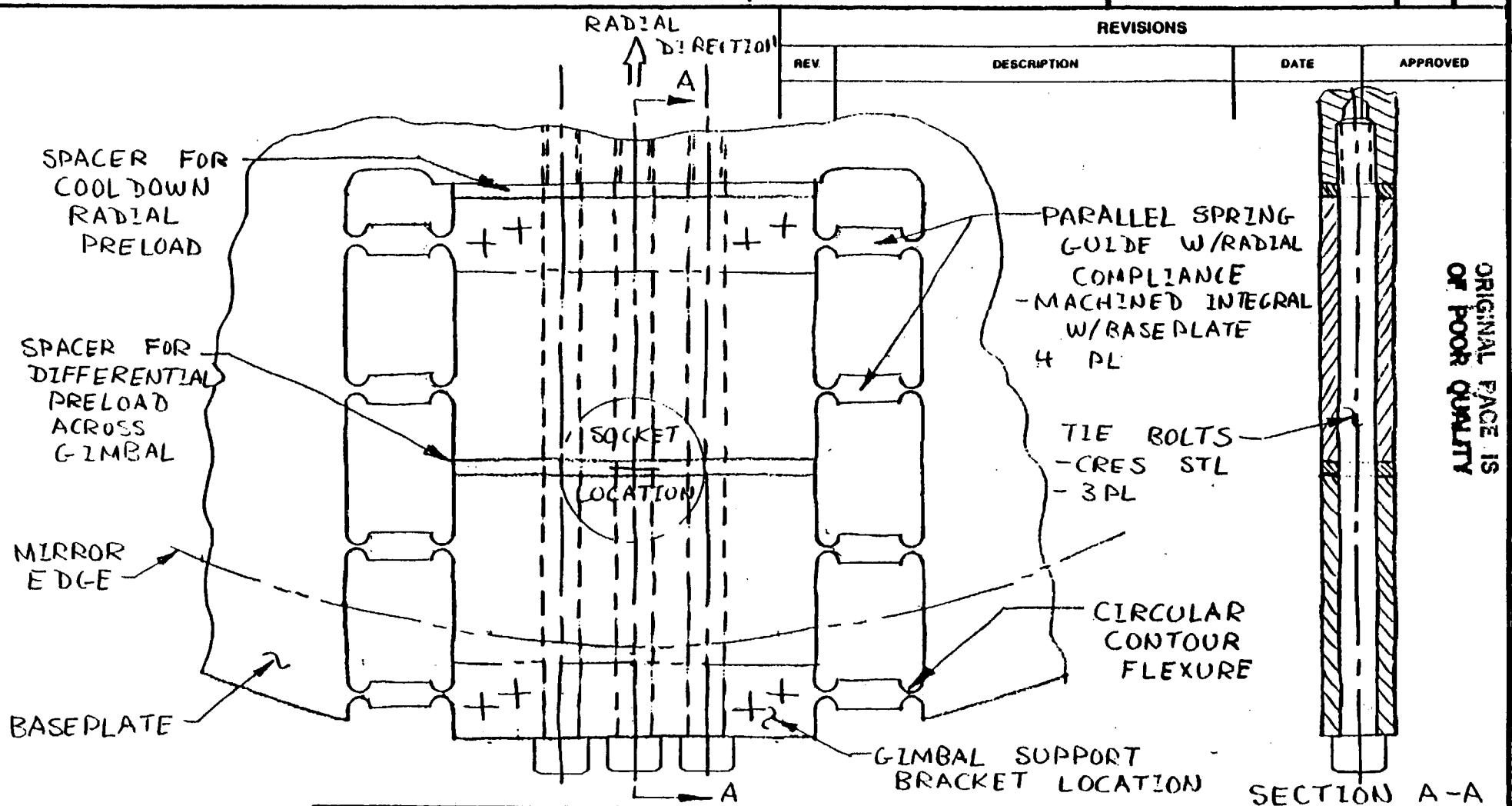

ORIGINAL FACE IS OF POOR QUALITY

Figure 30. Preloading Device

DWG. NO. 090486-10

REVISIONS			
REV.	DESCRIPTION	DATE	APPROVED

	QTY REQD	FSCM NO.	PART OR IDENTIFYING NO.	NOMENCLATURE OR DESCRIPTION	MATERIAL SPECIFICATION	

PARTS LIST

UNLESS OTHERWISE SPECIFIED DIMENSIONS ARE IN INCHES
TOLERANCES ARE:
FRACTIONS ± DECIMALS .XX ± .XXX ± ANGLES ±

MATERIAL

FINISH

NEXT ASSY | USED ON

APPLICATION

DO NOT SCALE DRAWING

CONTRACT NO. 881903

APPROVALS	DATE
DRAWN DV	10/20/86
CHECKED	
ISSUED	

OPTICAL SCIENCES CENTER
UNIVERSITY OF ARIZONA

NASA AMES DOUBLE ARCH MIRROR – PRELOADING FLEXURE

SIZE	FSCM NO.	DWG. NO.	REV.
A		090486-10	

SCALE FULL | SHEET

stresses for the design of the support system components. The equations used have certain simplifying assumptions contained within them that have been stated as they have been encountered. Those simplifying assumptions have allowed a closed form dynamic analysis to be performed that in turn allows parametric studies to be performed. Those resulting designs have been confirmed with the NASTRAN finite element program to be accurate within five percent. All designs required the use of NASTRAN to perform the stability analyses.

SUMMARY

Presented herein are the criteria and considerations for the design of the support system for the SIRTF primary mirror. A flexure-gimbal-baseplate design for the 0.5-m primary mirror model has been developed. Preliminary studies have indicated that this design may be further improved by replacing the flexures by a post-gimbal system wherein the gimbal design accommodates both the cryogenic cool down effects, the dynamic launch loads, and manufacturing tolerance effects. Additionally, a prestressed baseplate concept has evolved and has been presented for the full scale 1.0-m mirror. However, preliminary design studies indicate that this novel concept will not be required, and the post-gimbal-baseplate design similar to the 0.5-m alternate support system will meet the cryogenic cool down, dynamic launch load criteria, and manufacturing tolerance effects.

Appendix

Developmental History of Flexure-Mounted Mirrors for Use in Space Telescopes

Classical terrestial mirror mounts are not suitable for space telescopes. Differential thermal distortion and large mass generate the design criteria for these mounts. Three-point kinematic mounts reduce, but do not completely eliminate, these problems.

In 1964, Chin[1] described a three-point tangential flexure mount for use in a space telescope. A lightweight quartz mirror of egg-crate construction was supported by means of three points around its circumference. Cantilever flexures, located tangentially to the mirror edge, were attached by a spherical ball and socket to the mirror rib structure. This mount design reduced both the magnitude of the differential thermal stress on the mirror and the size of the moments that the flexure exerted on the mirror. Additionally, the stresses caused by misalignments during assembly were alleviated.

A 0.2 m conceptual model of this mounting system was vibration tested as part of the Orbital Astronomical Observatory Project. A maximum amplification factor of 11 was observed in the mount when excited at 230 Hz. The mount failed at a 300-g vibratory force.

In 1969, Jackson[2] reported on a tangent-bar-mounted 0.69 m diameter beryllium mirror intended for the OAO-B. The mirror was a thin solid meniscus, with three equispaced tangent bars attached to its circumference. The tangent bars were bolted at their midpoints to the mirror edge and provided radial compliance between the mirror and mounting structure. The use of tangent bars instead of cantilever flexures greatly increased stiffness of the mounted mirror. This mount and mirror survived 11.5 g steady state acceleration during test. A failure of the launch rocket prevented this system from reaching orbit.

In 1972,[3] an 0.89 m fused silica slotted egg-crate lighweight mirror mounted with cantilever tangential edge flexures was placed into orbit as part of the OAO-C. This mount system was similar to that described by Chin, and was caged during launch. Telescope performance in orbit was acceptable.

In 1975, Hog presented the theoretical advantages[4] of mounting mirrors by means of axial edge flexures. The flexures were to be parallel to the optical axis of the mirror to provide radial compliance to alleviate differential thermal distortion. Hog claimed that this type of flexure mount would be sufficiently precise to be used in astrometric instruments.

In 1980, the design of the Teal Ruby mirror support system was published by Pepi, et al.[5] The Teal Ruby primary mirror was a 0.5 m diameter lightweight fused silica mirror with a cellular core. Three equispaced mounting bosses were provided around the circumference of the mirror. Cantilever tangent flexures were attached to these mounting bosses by means of a leaf-spring subflexure system bonded to the mirror. This mount was conceptually similar to that described by Chin. The mirror was intended to operate at 70 K. The fundamental frequency of the mirror and mount was 45 Hz. The system survived both a 7-g steady state acceleration and a 10-g rms vibration test.

The IRAS satellite primary mirror mount was described by Schreibman and Young in 1980.[6] This was a ribbed-back or waffle-plate machined beryllium lightweight mirror. Cantilever flexures were attached to the back of the mirror at three equispaced points located on a common ring. The flexures were a 5A1-2.55n ELI titanium alloy and were parallel to the optical axis. The mount flexures were provided with additional torsional cruciform flexure system to attach to the mirror. The system operated at 2 K. IRAS was successfully operated in orbit for a year.

In 1981, French patent 8106724 was issued on a mirror mount using flexures edge-mounted by an intermediate 2-degrees of freedom cross strip gimbal.[7] This mounting scheme was identical to the one suggested by Hog in 1975. The U.S. patent, number

4,533,100, issued on August 6, 1985, makes no mention of any of the prior similar designs.

In 1983, Barnes analyzed the performance of a 0.66 m diameter cellular core fused silica lightweight mirror at 13 K.[8] This design was very similar to that used for the Teal Ruby design and consisted of invar cantilever flexures tangential to the mirror circumference and attached to edge bosses by a bonded leaf spring system. This was a developmental concept and was not deployed in a system.

Iraninejad, et al,[9] described in 1983 a 0.5 m diameter fused silica double arch mirror developed as part of the SIRTF program. This mirror was mounted using T-clamps and sockets in the back of the mirror by means of three equispaced parallel spring guides. The spring guides were parallel to the optical axis and were fabricated from 6A1-4V titanium. The mirror and mount system were successfully tested at 7 K.

Results of a feasibility study for ISO were presented in 1985 by Espiard, et al,[10] of a flexure-mounted cryogenic lightweight mirror. Zerodur was selected for the 0.6 m machined cellular core mirror. The mirror was mounted via three equispaced parallel spring guides attached at the circumference. The parallel spring guides were parallel to the optical axis and were fabricated from stainless steel. A 2-degree-of-freedom cross-strip flexural gimbal was provided between the top of the parallel spring guide and point of attachment to the mirror. This secondary flexure system provided moment isolation and relaxed the fabrication tolderances required. This design was intended to operate at 10 K.

German Infrared Laboratory personnel developed a lightweight double-tapered 0.5 m diameter Zerodur test mirror, as described by Schlegelmilch and Altman in 1985.[11] This mirror was intended to operate between 5 and 10 K. The mirror was mounted by means of three mushroom-shaped clamps and sockets in the back. The clamps were attached to a 2 degree of freedom leaf spring flexure system which in turn was bolted to an Invar subframe. The subframe was mounted to the telescope structure by three spring guides parallel to the optical axis. This complex mounting scheme was tested

under vibratory loading. The system had a transverse natural frequency of 108 Hz and an axial natural frequency of 230 Hz. Tests with 12-g acceleration at a maximum frequency of 35 Hz and a rate of charge of 3 octaves per minute did not damage the mounted mirror.

REFERENCES

1. Chin, D., "Optical Mirror-Mount Design and Philosophy," *Applied Optics*, Vol. 3, No. 7, July, 1964, pp. 895-901.

2. Jackson, B. W., "Structural Design for Large Space Telescopes," *Optical Telescope Technology, MSFC Workshop, April, 1969*, NASA Report SP-233.

3. Yoder, P. R., Jr., *Opto-Mechanical Systems Design*, Marcel-Dekker, New York, N. Y., 1986.

4. Hog, E., "A Kinematic Mounting," *Astronomy & Astrophysics*, Vol. 41, 1975, pp. 107-109.

5. Pepi, J. W., et al, "Teal Ruby-Design, Manufacture & Test," *SPIE Vol. 250, Optomechanical Systems Design*, 1980.

6. Schreibman, M., & Young, P., "Design of Infrared Astronomical Satellite (IRAS) Primary Mirror Mounts," *SPIE Vol. 250, Optomechanical Systems Design*, 1980.

7. U. S. Patent No. 4,533,100, Aug. 6, 1985, Issued to Jacques Paserl, "Mounting Device for Supporting a Component, Especially a Mirror or an Antenna Reflector in a Spacecraft."

8. Barnes, W. P., Jr., *Fused Silica Mirror Development for SIRTF*, NASA Contractor Report 166522, July, 1983.

9. Iraninejad, B. et al, "A Mirror Mount for Cryogenic Environment," *SPIE 450, Structural Mechanics of Optical Systems*, 1983.

10. Espiard, J., et al, "Lightweight Cold Mirror and Fixation," *SPIE Vol. 589, Instrumentation for Optical Remote Sensing from Space, 1985.*

11. Schlegelmilch, R., and Altmann, J., "A Cooled Infrared Telescope for the Girl German Infrared Laboratory," Zeiss Information, *No. 96, Vol. 28, Dec. 1985, pp. 19-23.*